

Design and Validation of a Novel Mission Framework for the Detumbling of Rotating Space Debris Using a Tether-Net Linkage and Momentum Wheel

Worcester Polytechnic Institute

Authors: Josh Desmond, Max Luu, Tim Stump

Advisors: Frank Dick, Zhikun Hou, Carlo Pincioli

Table of Contents

Table of Contents	1
Abstract	3
1 Introduction	4
2 Background	6
2.1 Target Space Debris and the Low Earth Orbit Environment	6
Kessler Syndrome	6
Low Earth Orbit	6
2.2 Debris Tumbling Due to Environmental Torques	8
Gravitational Torque	8
Aerodynamic Torque	8
Solar and Electromagnetic Radiation Torque	8
2.3 Summary of Active Debris Capture and Removal Methods	9
2.4 Contactless Methods	9
2.5 Stiff-Connection Methods	9
2.6 Flexible-Connection Methods	10
2.7 Review of Tether-Net Capturing Methods	10
2.8 Use of Momentum Wheels in Spacecraft	13
2.9 Simulation of Tether-Net Capture Methods	13
3 Design	15
3.1 Problem Formulation	15
3.2 Mission and Theoretical Spacecraft Design	15
General Aspects	15
Orbital Inclination and Orbital Parameter Changes	16
Spacecraft Design	17
Propellant Calculations	17
Power Subsystem	20
Mission Mass Breakdown	22
3.3 Experimental System Design	22
Net Simulation Design	22
Tether-Net Experimental Design	25
Mechanical System Design	25
Electrical System Design	27
Chaser Electrical System	27
Target Electrical System	28

Software Design	28
Target Software Design	28
Target Software Design	29
4 Experimental Results	30
4.1 Net Simulation Experiment	30
4.2 Tether-Net Experiment	32
Setup	32
4.3 Results and Discussion	34
5 Concluding Remarks	37
5.1 Conclusions	37
5.2 Lessons Learned	37
5.3 Suggested Future Work	37
Works Cited	39

Abstract

Space debris in low Earth orbit (LEO) is a growing concern for the future of space travel and current satellite use. As the number of artificial satellites in LEO increases, the probability of collisions between these artificial satellites increases, and so does the need for cost-effective space debris remediation. In this project, we designed and tested a mission framework for the capture and detumbling of space debris. A computer simulation was used to observe the contact dynamics of a net on space debris and its efficacy in capturing tumbling satellites. An experiment was designed and executed to validate the use of a momentum wheel and tether-net linkage to detumble spinning space debris. Through simulation and experimentation, it was shown that controlling a piece of tumbling debris with a tether-net connection and momentum wheel is a feasible solution for low-mass debris removal mission.

1 Introduction

Space operations in Earth's orbit are under increasing threat from space debris. Space debris consists of rocket bodies, dead satellites, and any artificial object that was discarded or accidentally produced in Earth's orbit (Imburgia, 2011). Much of space debris was created from collisions or explosions. In 2007, there were over 15,000 objects being tracked in Earth's orbit that have the capability of causing catastrophic damage to space assets if they were to collide (Pulliam, 2011). The amount of space debris is constantly increasing. During 2017, 1017 new objects were added to Lower Earth Orbit (LEO). This constant addition of space debris is feared to lead to the Kessler Effect, a phenomenon coined by Donald Kessler and Burton Cour-Palais in which collisions between pieces of space debris would cause a chain reaction ending in a debris belt around Earth. This would make space operations extremely difficult (Kessler et al., 2010).

To prevent this event, space debris remediation is necessary. After running simulations dealing with the accumulation of space debris in LEO, NASA determined that along with post mission-disposal of 90% of satellites currently in LEO, five of the largest pieces of debris will need to be removed annually to inhibit space debris levels from growing (Pulliam, 2011). Although there has been a great deal of research into methods of space debris remediation, no debris has been deorbited yet (Shan et al., 2016).

Contactless, stiff-connection, and flexible-connection methods have all been proposed by researchers for space debris remediation and all exhibit their own advantages and disadvantages. Contactless methods avoid the challenge of latching onto rotating space debris with unknown attachment points. Instead they use lasers, ions, or chemical propellants to gently slow down space debris using various particles as a way to transfer momentum. These techniques are still very early in their research, however, and take an extended amount of time to deorbit debris because of how weak they are (Shan, Guo, & Gill, 2016; Bombardelli & Pelaez, 2011). Stiff-connection methods use mechanical grippers or robotic arms to latch onto debris so that the debris is able to be manipulated by the satellite. It is difficult for stiff-contact methods to capture a wide range of debris types for some may be rotating too fast or have no ideal location for the satellite to grab onto (Shan, Guo, & Gill, 2016). Flexible-connection methods are able to capture a wide range of debris types and states. They often use tethers to apply forces and torques to slow down debris and deorbit it. The tethers are attached to the debris either through mechanical grippers or nets (Shan, Guo, & Gill, 2016; O'Connor & Hayden, 2017). Tether-Net capture methods are one of the more promising approaches.

This paper explores the tether-net capture method. Tether-net space debris remediation methods can handle a wide range of debris sizes and shapes. It can also handle rotating debris fairly well, making it a prospective method for removing debris (Shan, Guo, & Gill, 2016).

A mission framework was designed for a satellite that could change its orbital inclination and radius four times and detumble five unique pieces of debris. To do this, assumptions on the satellite's dry mass were made to find a total required ΔV , or the total required velocity (provided by the propulsion system on the satellite) to change orbit four times for our mission. After finding the initial ΔV , a primary propulsion engine was chosen based on minimizing final propellant mass, and a electric power system for the detumbling mechanism was chosen based on high-power solar cells. Mass estimates were found for the different subsystems and a total spacecraft wet mass was estimated.

To explore this mission framework, two separate experiments were conducted. The first dealt with studying the capture dynamics of a net around an object in zero gravity. A simulation using Bullet Physics¹ was created of a net using a mass-spring-damper model. To test the accuracy of this simulation to the real world, a physical net dropping on an object was mapped using an infrared Vicon camera system². The second experiment used two freely rotating platforms aligned along the same axis of rotation, one above the other, to represent a chaser satellite and space debris. The chaser satellite platform holds a motor with a momentum wheel attached, that is able to be accelerated and in return apply a torque to the system to represent the detumbling of the space debris. These two platforms were attached with a rigid connection, tether connection, and tether net connection so that the behavior of each connection type was able to be studied.

¹ <https://pybullet.org/wordpress/>

² <https://www.vicon.com/>

2 Background

2.1 Target Space Debris and the Low Earth Orbit Environment

Kessler Syndrome

Space debris in low Earth orbit (LEO) is a growing concern for the future of space travel and current satellite use. As the number of artificial satellites in LEO increases, the probability of collisions between these artificial satellites increases. Donald Kessler and Burton Cour-Palais' 1978 paper, titled *Collision frequency of artificial satellites: The creation of a debris belt*, describes a case in which satellite collisions would produce "orbiting fragments, each of which would increase the probability of further collisions, leading to the growth of a belt of debris around the Earth." In their paper, a mathematical simulation was executed that concluded that, by the year 2000, space debris density would be so high that random collisions would begin occurring in Low Earth Orbit (LEO). Unintentional high-speed collisions between active satellites began in 1996, with the collision between the French Cerise military reconnaissance satellite and debris from an Ariane rocket. In 2009, a collision between the Iridium 33 communications satellite and a dead Russian Kosmos 2251 communications satellite resulted in the complete destruction of both satellites, creating a large amount of debris. In 2010 alone, four separate satellites conducted avoidance maneuvers to avoid debris from the 2009 collision between the Iridium and Kosmos satellites (UNOOSA NASA Presentation, 2011).

Low Earth Orbit

The low Earth orbit environment, defined by the NASA Orbital Debris Office as the region between 200 km and 2000 km in altitude, holds the highest risk for a Kessler event in the near future. A 2011 DARPA study headed by Wade Pulliam identified future collision rates using a Monte Carlo simulation for low Earth orbit, middle Earth orbit (MEO - 2000 km - 35,586 km altitude), and geostationary orbit (GEO - 35,586km - 35,986km), shown in Figure 1. With 178 predicted collisions in LEO and a total of 5 collisions in MEO and GEO, it is clear that debris mitigation efforts should focus on the LEO environment.

Ave. collisions in the next 200 years (non-mitigation scenario)			
	Cat.	Non-cat.	Total
LEO	83	95	178
MEO	0.5	1.5	2
GEO	1.5	1.5	3

Figure 1. Average collisions predicted in the next 200 years based on altitude (NASA, 2005)

According to a NASA Orbital Debris Office simulation using a Monte Carlo simulation method, about 60% of predicted collision events occur between 900 and 1000 km in altitude in LEO (Figure 2), with 85% of trackable debris in LEO collected between 750 km and 1050 km (Liou, 2011).

At the current rate, NASA predicts that an orbital collision involving a functional satellite will occur once every five years, with an increasing rate as time progresses (Pulliam, 2011).

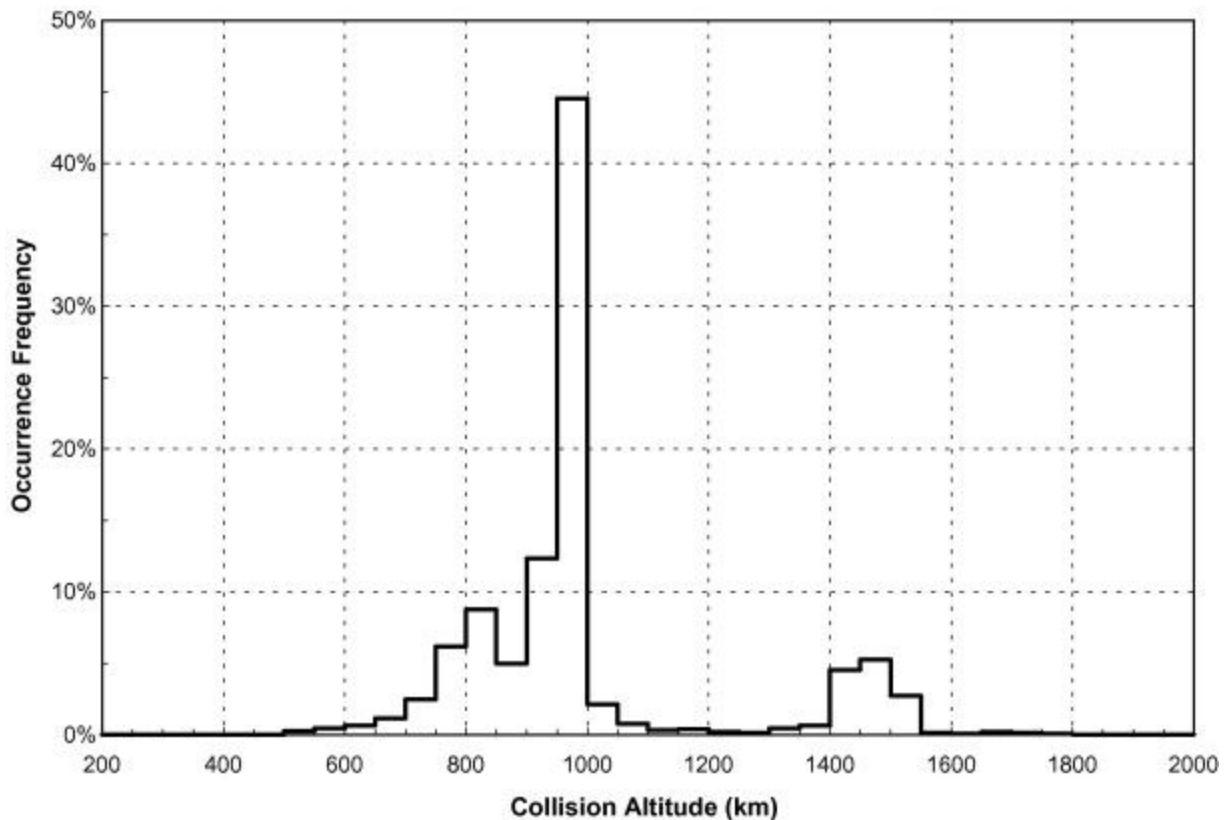


Figure 2. Distribution of predicted catastrophic collisions as a function of altitude (Liou, 2011)

2.2 Debris Tumbling Due to Environmental Torques

The three largest external torques spacecraft experience over time in orbit are the gravity gradient effect on non-isotropic shaped satellites, aerodynamic torque (drag), and electromagnetic radiation torque due to Earth's magnetic field and solar radiation pressure (Hughes, 1986). When combined, these forces act on dead satellites and debris to induce rotation and tumbling motion (Hughes, 1986).

Gravitational Torque

Torque induced by the gravity gradient torque depends on the physical properties and orbit characteristics of the spacecraft. Earth's gravitational force is inversely proportional to the square of the distance to the center of gravity of the planet. Due to this relationship, the gravity gradient torque affects non-isotropic shapes based on their mass distribution and inertial tensor (Gomez, Walker, 2015).

Aerodynamic Torque

Satellites experience different forces due to aerodynamic drag through the thin atmosphere in LEO based on their shape. In his 1994 paper, E.M. Gaposkin describes methods for calculating drag coefficients based on the shape of the satellite. Using the drag coefficient, speed of the satellite in relation to Earth, mass of the satellite on Earth, atmospheric mass density, and cross-section perpendicular to the atmospheric drag, the magnitude and position of the atmospheric drag force on a satellite can be calculated.

Solar and Electromagnetic Radiation Torque

Both the magnetic field and solar radiation pressure are "frequently the dominant external influence on spacecraft attitude" (Hughes, 1986). As Gomez and Walker note, "Due to the existence of an external magnetic field from the Earth, the rotation of the object induces electric currents following Lenz's Law. These currents are responsible for a dissipative effect caused by Joule's Law which translates into a torque that opposes to the general rotational movement of the object" (Gomez & Walker, 2015). Solar radiation pressure affects satellites depending on the albedo of the object and the position of the satellite with regards to the Sun. Over time, the radiation torque on a satellite increases: "the magnitude of the radiation-pressure torque will be influenced by the nature of the satellite's surface, i.e. whether the surface reflects or absorbs most of the radiation. Bombardment by cosmic dust (micrometeorites) over a long time will inevitably produce a gradual erosion of the outer metallic skin of the satellite, similar to the erosion of a metal by the impact of high-speed molecules" (Ives et al., 1963). In a 2015 case study, Gomez and Walker calculated the rotational dynamics of Envisat, finding that both gravity gradient and radiation torque caused multiple changes to spin rate and precession about the axis of rotation after simulating torques on Envisat over a time period of 20 days (Gomez & Walker, 2015).

2.3 Summary of Active Debris Capture and Removal Methods

Many techniques have been proposed within the scientific community to clean up debris in Low Earth Orbit. The capture and removal of a targeted debris requires planning for at least five different phases of the mission (Shan et al., 2016). This includes the launch and early orbit phase, the long-range rendezvous with the debris, the close-range rendezvous and flight synchronization, capture phase, and removal phase. The designs and plans to remove space debris can be categorized into contactless, stiff connection, and flexible connection methods. The need for such a variety in capture methods stems from the wide range of debris types that may be found in LEO with varying sizes, shapes, and rotational dynamics. Even though many plans have been developed, not a single piece of debris has been removed yet, increasing the importance of future research in this field (Shan et al., 2016; Wormnes et al., 2013).

2.4 Contactless Methods

Contactless methods avoid the complication of attaching to a targeted debris whose physical state and attitude may be unknown. Instead, they utilize the transfer of momentum to slow down debris into a graveyard orbit. For example, ion beams, lasers, or chemical propellants are aimed at a piece of debris to gently decrease its velocity, causing it to fall out of orbit. Since these methods use miniscule particles to apply relatively small forces to the target, it takes a substantial amount of time to slow the target's velocity enough to deorbit it. This means that the debris and chaser satellite have the risk of impacting other debris over the course of its long deorbit procedure. Additionally, the larger the piece of target debris, the longer a contactless method will take to deorbit it. The ion beam shepherd method, for example, is best used on relatively small debris, under 100 kg (Wormnes et al., 2013). There are many unknowns that require future research for these methods of debris removal, such as the influence of sputtering ions on the chaser satellite when reflected (Shan et al., 2016).

2.5 Stiff-Connection Methods

Stiff contact methods use mechanisms to firmly attach to the space debris so that they may apply force, from thrusters, to stop the debris' rotation and slow it down. Robotic arms, grippers, and tentacles have been proposed as attaching mechanisms. These methods are advantageous because of their capability of being tested on the ground before being implemented in space. Robotic arms have also been used in space missions already, but for attaching to controlled objects. All stiff contact approaches face problems regarding a complex rendezvous phase where the chaser satellite has to match the target's velocity, attitude, and rotation before attempting to grab the debris and potentially bouncing off. This is further

complicated because the target's mass, rotational dynamics, and attitude are often unknown. Because of this, these methods are best used on space debris that is not tumbling or uncontrolled (Shan et al., 2016).

2.6 Flexible-Connection Methods

Flexible capture methods apply forces and torques through a tether to slow down and deorbit space debris. The tether is attached to the targeted debris by either launching a net, harpoon, or mechanical gripper at the debris. Because the chaser satellite does not need to fully synchronize its rotation with the debris' rotation to capture it, flexible methods can be used on a wider range of debris tumble rates. Nets also do not need a specified location to grab onto such as a robotic arm would, so the physical properties of the debris do not need to be known beforehand. Controlling a piece of debris via tether is more complicated than a stiff connection method, however, and require more complex controls (O'Connor & Hayden, 2017). These methods also have a larger risk of breaking off parts of the debris during the capture phase (Shan et al., 2016).

2.7 Review of Tether-Net Capturing Methods

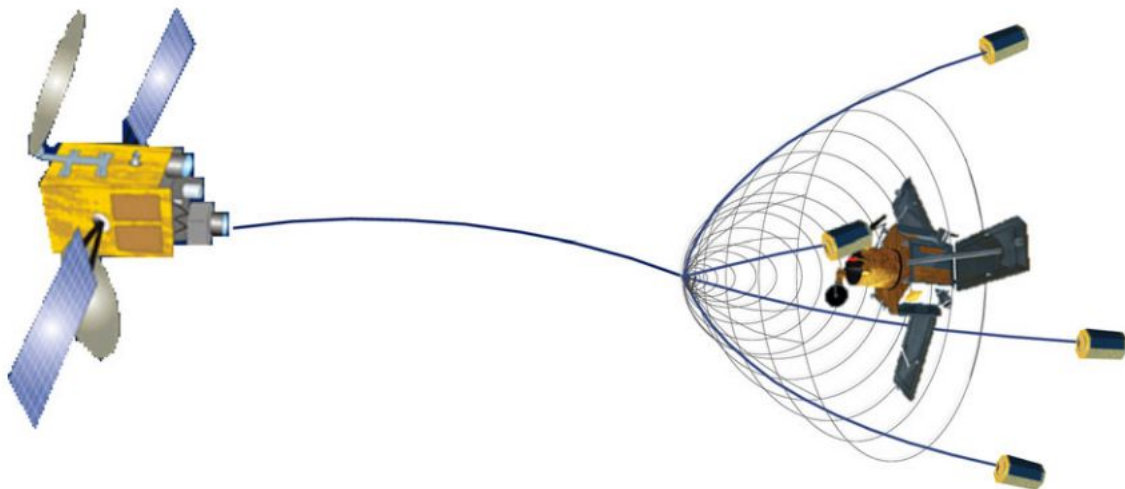


Figure 3. Satellite capturing debris utilizing the tether-net method (Huang et al., 2018)

Our project is based on the use of a tether-net mechanism for capturing and controlling debris. The technique of tether based capturing methods requires first capturing the debris and connecting it to a chaser satellite with an elastic tether. Figure 3 shows a debris once it has been captured.

Once debris has been captured, it is possible to control the attitude of and detumble the debris using only forces applied via tether (O'Connor & Hayden, 2017; Wang, Meng, & Huang, 2017; Aslanov & Yudin, 2013). The chaser satellite would be equipped with thrusters, which are able to counteract the torque applied to the tether from the rotation of the captured debris. Thrusters on the chaser satellite are also responsible for applying the force required to slow the debris to cause it to deorbit. The amount of tension on the tether can also be managed via a reel mechanism; this means the chaser would be able to control the tether length by reeling in or out tether (Wang, Meng, & Huang, 2017). The reel mechanism, in combination with the elasticity of the tether, prevents collisions between the chaser and debris while controlling rotational dynamics of the target debris.

The physical characteristics of the tether play a key role in how the overall system of the chaser and debris will act once attached. The tether length and elasticity determine the dynamics of controlling the space debris. A stiffer and shorter tether will allow for more sensitive control of the captured debris because of its ability to translate forces faster. A short tether, however, might also increase the chances of a collision with both satellites. A more elastic tether in both the lengthwise and torsional direction allows the chaser satellite to apply force more slowly, allowing time to adjust controls (O'Connor & Hayden, 2017). A tether that is too elastic would be unstable and could result in the chaser and debris being launched into each other (Shan, Guo, & Gill, 2016).

One of the greater concerns to using a tether is the possibility of the tether wrapping around a tumbling debris. This would cause a large disturbance in the system when the tether eventually unfurls. O'Connor and Hayden addressed this problem in their simulations of controlling debris with tethers. They simulated a large disturbance in the model which represents the sudden tautness of the tether after becoming untangled. Their system handled this problem fine without loss of control or breakage. Real parameters were also simulated to find the likelihood of the tether wrapping around the debris. O'Connor and Hayden found that the likelihood of the tether entangling the debris was low and that to even make one full revolution around the debris required a large angular velocity and low tether stiffness (O'Connor & Hayden, 2017). Tether control of rotating space debris is a feasible approach for active debris removal.

The general approach for net capture is to have weighted masses on the corner of the net. The net is launched, and spreads open via centrifugal forces (Huang et al., 2018). The launch of the corner bullet masses propels the net forward until contact is made with the target debris. Once contact is made, the bullet inertia will cause them to continue to travel around the target debris and wrap around it. The design choices involved with net shape, mesh topology, material, and deployment mechanism have been studied extensively (Zhao, Huang, & Zhang, 2018).

Many factors dictate the success of a net capturing a piece of space debris. A net must hold a desired shape before coming into contact with the target to assure a proper capture. The actual shape of the net depends on variables such as the masses of the bullets, the velocity it is launched at, and the mesh topography. Huang found that square mesh is the best mesh for

pre-stressibility under centripetal forces. The net may open as it is launched due to the direction of the velocity of the bullets as well as the centripetal force created from the net rotating (Huang et al., 2018). Net size, bullet masses, and launch velocities are easily scalable based off of the size of debris, making net capture very adaptable to debris type (Benvenuto & Lavagna, n.d.). Some net designs include cinch cords to assure the net fully captures debris by enclosing around it like a drawstring bag. O'Connor and Hayden simulated a design where the cinch cords are looped around the perimeter of a net and attached to the tether so that when the tether stiffens, it closes the net. Their net design worked better than general space nets as it did not fall off the space debris in simulations (O'Connor & Hayden, 2017).

The Maneuverable Tethered Space Net Robot (MTSNR), proposed by Zhao, Huang and Zhang, is a unique net-robot configuration which consists of a square net with a maneuverable robot at each vertex (Zhao, Huang & Zhang, 2018). Having a maneuverable unit at each corner allows the net to be controlled to a higher degree of accuracy when compared to the standard space net. The 3D orientation of the net may be altered to better cope with the specific debris type and rotation. The maneuverable units may even apply thrust and adjust their direction during the entrapment of the targeted space debris to more securely capture it (Zhao, Huang, & Zhang, 2018). The control of multiple satellites, however, is more complicated and long distance flights are difficult and consume more fuel. The formation of tethered space robots can be controlled with the tether tension, thrusters, and reaction wheels creating gyroscopic stabilization and attitude control. The square formation as well as triangle formations can even fly in a rotating formation around an axis tangent to the plane of the satellite's orbits. Tethered space robots are a relatively new field and still require further research of the unfolding of the formation, reconfiguration of the system in flight, and controlling the formation when treating the tethers as having both mass and elasticity (Huang et al., 2018).

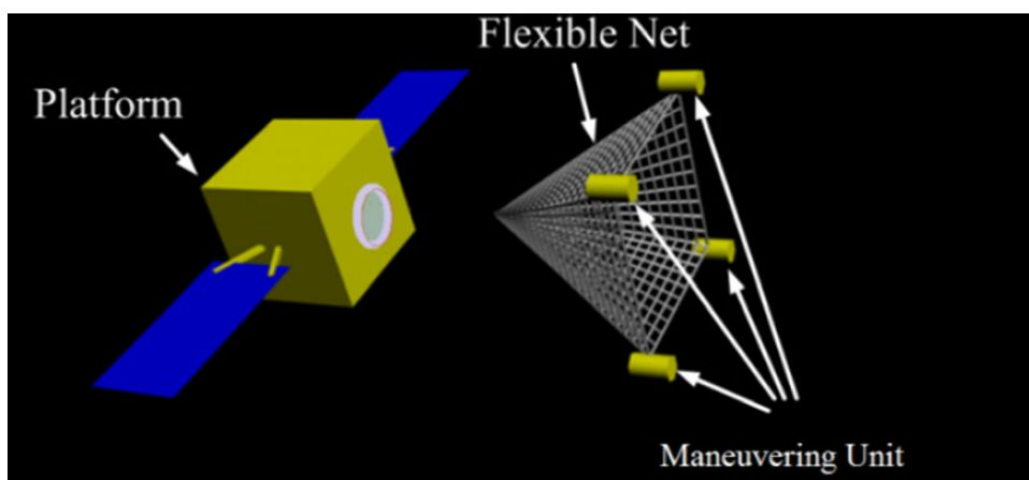


Figure 4. MTSNR diagram displaying the use of maneuvering units with a net (Zhang & Huang, 2018)

2.8 Use of Momentum Wheels in Spacecraft

Momentum wheels are commonly used in spacecraft to control their attitude. The rotation of a momentum wheel is able to rotate a satellite because of Newton's First law and the conservation of momentum. Often satellites that use momentum wheels for attitude control will have three, one wheel aligned with each respective axis (Krishnan, McClamroch, & Reyhanoglu, 1995). Some designs use the momentum wheel for both attitude control and energy storage. Momentum wheels are advantageous to batteries for storing and releasing energy since batteries also require extra power during the charging and discharging phases (Tsiotras, Shen, & Hall, 2001).

2.9 Simulation of Tether-Net Capture Methods

The tether-net system consists of multiple flexible bodies and their collision and contact with other bodies. The behavior of the system is complex and nonlinear. As such, creating an simulation to model the contact dynamics of net capturing is an ongoing challenge. Simulations of nets make assumptions which simplify the mathematics of describing nets' behavior, at the cost of accuracy.

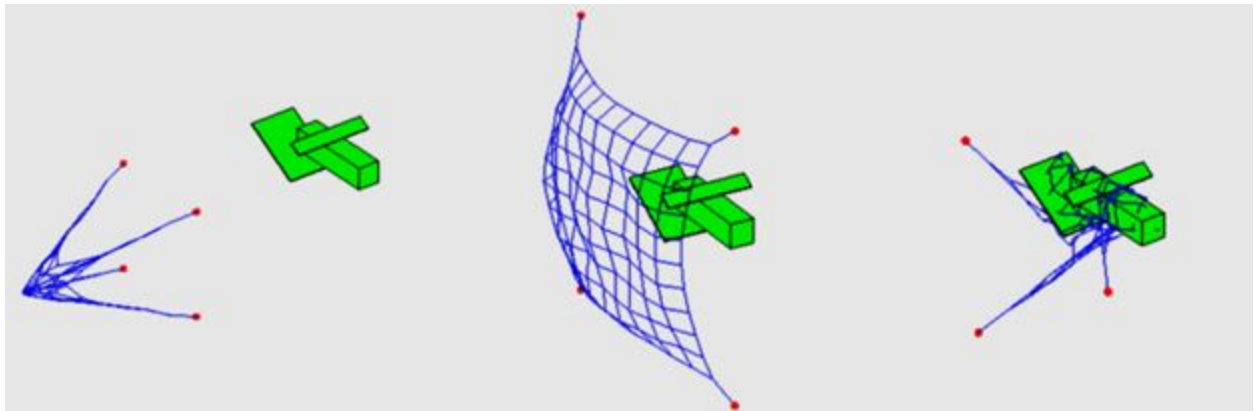


Figure 5. A simulation of the net capturing process from Shan, Guo, & Gill, 2018

The mass-spring-damper model is the basic approach used for the basis of many simulations (Shan, Guo, & Gill, 2018; Botta, Sharf, Misra, & Teichmann, 2016; de Jong, Wormnes, & Tiso, 2014). In the model, mass is distributed across individual nodes, which are placed at the corners or intersections of the net, and mass points are connected via spring dampers. Spring dampers are elastic connections which resist compression but exhibit elasticity through spring action. The use of this spring-dampers is also described as a finite element model (Yang, Zhang, Zhen, & Liu, 2017).

In contrast, Gołębiowski et al. has reported on the development of a simulation engine based around the Cosserat Rod Theory (Gołębiowski et al., 2014; 2016). This method attempts to use nonlinear dynamic models to better capture the behavior of the net in regions experiencing high amounts of stress (Gołębiowski et al. 2016; Cao & Tucker, 2008). Gołębiowski's work is based around the development of a new simulation engine, ADRiNET. A public release is not yet available.

There have been a few attempts to validate simulations using parabolic flight experiments that emulate a zero gravity environment. Gołębiowski et al. and Shan both validated their models of net deployment and contact using one parabolic space experiment (Gołębiowski, et al. 2016; Shan, Guo, & Gill, 2017). Benvenuto's 2016 work on simulation based on the mass-spring-damper model was validated in another parabolic flight experiment (Medina et al., 2017).

Different papers have relied on different software suites to execute simulations. Work done by Botta et al. and Sharf have tested simulation models built on the commercial software, Vortex Dynamics (Botta et al., 2016; Sharf, 2017). A non graphical simulation of the controls and forces was created by O'Connor using MATLAB's Simulink software (O'Connor, 2017). The PATENDER software described in Medina et al.'s 2017 work relies on both MATLAB's Simulink to propagate the system, a collision detection algorithm based on the Bullet Physics engine, and on Blender/OpenGL engine for visual rendering. The ADRiNET simulation engine was built from scratch, but relies on Bullet Physics only for collision detection.

3 Design

3.1 Problem Formulation

According to DARPA's Catcher's Mitt report, if five of the largest pieces of debris are removed from LEO per year and satellite launches adhere to strict post-mission disposal, debris density can be stabilized in LEO (DARPA, 2009). Our proposed satellite would have the ability to detumble five large pieces of debris with contingency propellant left for deorbiting. Additionally, our proposed detumbling system would not create more debris from impacts. Two hypothetical targets, LANDSAT-4 and LANDSAT-5, were chosen for their orbital and mass characteristics. For the purpose of designing an ideal mission, a fully electric detumbling that requires no propellant to detumble the debris is proposed. Additionally, a launch is assumed to place the satellite into a close trailing orbit for the first piece of debris.

3.2 Mission and Theoretical Spacecraft Design

General Aspects

We propose a mission framework and spacecraft design for a debris-capture satellite, taking in to account multiple phases of a mission. Our proposed system would have the ability to detumble five unique large satellites (with an outside satellite assumed to deorbit each stationary, orbiting piece of debris), which, if successful, could stabilize the debris density in LEO (DARPA, 2011). We chose a momentum wheel to detumble the debris. A momentum wheel is a simple way of creating a large quantity of angular momentum and is commonly used in spacecraft for attitude control. To capture the debris, we chose a tether-net system due to a high success rate for capture, simple simulation and experimentation, and ability to capture debris without creating new debris (as mentioned in Section 2.7, Review of Tether-Net Capturing Methods). A satellite dry mass (not including power and propulsion subsystems) is assumed to be 100kg. This includes wiring, structure, processing and memory unit, and detumbling subsystem. A preliminary satellite wet mass was calculated using ΔV budget and power requirements to show low-mass solutions to large, tumbling debris are feasible.

Our designed mission would consist of three phases: launch, detumbling phase, and self deorbit. The launch phase would place the satellite into a close trailing orbit for the first piece of debris. The second phase, deorbit, would begin by first capturing and detumbling the first piece of debris using the tether-net method. This phase is the most crucial, due to the high possibility for failure and the untested nature of deorbit methods. After detumbling, the spacecraft would detach the net and a second spacecraft (the deorbitSat) would attach to and deorbit the debris (attaching to stationary debris is far simpler than tumbling debris). After detaching the net from the debris, the spacecraft would begin its Hohmann transfer to the next target debris, repeating

four times until the spacecraft is nearly out of propellant. After finishing the detumbling phase, the spacecraft deorbit itself to burn up in the atmosphere for its final phase.

Orbital Inclination and Orbital Parameter Changes

To find the total ΔV required by the mission, we calculated four arbitrary inclination changes. Orbital inclination and both perigee and apogee change were calculated for a transfer between two defunct satellite orbits (measurements taken in April 2019), from LANDSAT-5 to LANDSAT-4, using Edelbaum's model for low-thrust transfer between non-planar, concentric orbits (NORAD, 2019 ; Edelbaum, 1961).

Physical Constants and Parameters:			
Central Body:	Earth		
mu=	398611.32	km ³ /s ²	Grav Parameter
rpl=	6378.14	km	Planet Radius

Figure 6. Earth constants used for transfer calculations (Wertz, 2011)

Orbit A			
	Altitude (km)	Radius (km)	Velocity (km/s)
Periapsis:	535.60	6913.74	7.628
Apoapsis:	662.80	7040.94	7.490
Inclination:	98.1 deg		
	1.712 radians		
General Orbit Parameters			
Semi-major Axis:	6977.34 km		
Eccentricity:	0.009		
Spec Ang Mom:	52735.34 km ² /s		
Spec Mech Energy:	-28.56 km ² /s ²		
Period:	5.800E+03 sec		
	96.67 min		
	1.61 hrs		
Mean Motion:	1.08E-03 rad/sec		

Figure 7. Orbit parameters of LANDSAT 5 (NORAD, 2019)

Orbit B			
	Altitude (km)	Radius (km)	Velocity (km/s)
Periapsis:	513.0	6891.14	7.61103477
Apoapsis:	533.0	6911.14	7.58900936
Inclination:	98.2 deg		
	1.713913325	radians	
General Orbit Parameters			
Semi-major Axis:	6901.14	km	
Eccentricity:	0.001		
Spec Ang Mom:	52448.7	km ² /s	
Spec Mech Energy:	-28.88	(km/s) ²	
Period:	5705.40	s	
	95.09	min	
	1.58	hrs	
Mean Motion:	1.10E-03	rad/sec	

Figure 8. Orbit parameters of LANDSAT 4 (NORAD, 2019)

$$V_a^2 + V_b^2 - 2V_a V_b \cos\left(\frac{\pi\theta}{2}\right)^{\frac{1}{2}}$$

Figure 9. Edelbaum's model for low-thrust orbital changes (Wertz, 2011)

In Figure 9, variable V_a represents the orbital velocity of LANDSAT-5, and V_b represents the orbital velocity of LANDSAT-4, while θ represents the orbital inclination change between the two orbits in radians. Using Edelbaum's model for low-thrust orbital changes (Figure 9), a ΔV of 43.88 m/s was found for a single orbital transfer. From that calculation, total ΔV required for four orbital transfers was extrapolated to 175.5 m/s. With a factor of safety of 1.5, we calculated the total mission ΔV to be 263.25 m/s.

Spacecraft Design

Propellant Calculations

With a total mission ΔV of 263.25 m/s, both chemical and electric primary propulsion systems were considered, and are summarized in the below tables.

Chemical Propulsion Options

Thruster	Propellant Type	Specific Impulse I_{sp} (sec)	Mass (kg)	TRL
MR-111C	Hydrazine	220	1	9
MR-103M	Hydrazine	221	0.15	9
AR-1N	Hydrazine	220	0.29	9
AR-20N	Hydrazine	230	0.65	9
DST-11H	Hydrazine	310	0.77	9
DST-13	Hydrazine	298	0.68	9

Table 1. Small chemical monopropellant propulsion options with technology readiness level (MOOG Defense, 2019)

Electric Propulsion Options

Thruster	Propellant	Min/Max Power Per Thruster (kW)	Specific Impulse I_{sp} (sec)	Mass (kg)	TRL
Ion	Xenon	1.0 - 2.5	3300	12.0	9
Hall (high power)	Xenon	1.0 - 4.0	1800	20.0	9
Hall (mid power)	Xenon	0.2 - 0.6	1550	15.0	9
Hall (high power)	Xenon	0.1 - 0.2	1370	12.0	9
Arcjet	Hydrazine	1.0 - 1.8	500	5.6	9
Pulsed Plasma Thruster	Teflon	0.05 - 0.1	1150	4.7	9

Table 2. Small electric propulsion options with TRL (Technology Readiness Level) (Wertz, 2011)

Using the parameters from Tables 1 and 2, we used Tsiolkovsky's rocket equation with a ΔV of 263.26 m/s (with a contingency factor of 1.10) and a dry mass of 100kg to find propellant mass for chemical propellant.

Rocket Equation:		
Isp=	220.00 sec	Specific Impulse
Mo=	112.99 kg	Initial Wet Mass
Delta_V=	263.25 m/sec	Delta-V
Mf=	100.00 kg	Final Mass
Contingency Factor	1.10	
Mp=	14.29 kg	Propellant Mass
I_Total=	30799.58 N-sec	Total Impulse

Figure 10. Calculations using mission parameters, MR-111C characteristics, Tsiolkovsky's rocket equation (Figure 11)

$$\Delta v = v_e \ln \frac{m_o}{m_f} = I_{sp} g_0 \ln \frac{m_o}{m_f}$$

Figure 11. Tsiolkovsky's rocket equation (Wertz, 2011)

Propellant Mass for Thruster Options

Thruster	Propellant type	Specific Impulse (sec)	Propellant Mass (kg)
MR-111C	Chemical	220	14.29
MR-103M	Chemical	221	14.22
AR-1N	Chemical	220	14.21
AR-20N	Chemical	230	13.63
DST-11H	Chemical	310	9.96
DST-13	Chemical	298	10.38
Ion	Electric	3300	0.90
Hall (high power)	Electric	1800	1.65
Hall (mid power)	Electric	1550	1.92
Hall (high power)	Electric	1370	2.18
Arcjet	Electric	500	6.07
Pulsed Plasma Thruster	Electric	1150	2.60

Table 3. Propulsion options with calculated propellant mass (Wertz, 2011)

From Table 3 it was shown that, if choosing a chemical propulsion option, the DST-11H has the lowest propellant mass while still remaining below 1kg. For electric propulsion, the ion engine has the lowest propellant mass and the highest specific impulse, though it can consume up to 1kW during operation. For mission simplicity, the DST-11H monopropellant hydrazine thruster was chosen for the mission operations, with a mass of 0.77kg and a propellant mass of 9.96kg.

Power Subsystem

The power subsystem was calculated using estimates found from experimentation (this is discussed further in the Electrical System Design portion of this section). The main power draw in the satellite is the detumbling subsystem, which uses an electric motor to power a flywheel. Our experimentation used a 1.696kg flywheel and a 7kg piece of debris, and each detumbling cycle used a maximum of 20V at 0.5A. With an efficiency of 0.90, the power of the motor was 9W. Extrapolating to full-sized piece of debris at 2200kg, (in this case we use LANDSAT-5 as an example), a flywheel with a mass of 60kg would be used, and the power draw of the motor could reach up to 1.9kW per detumbling cycle. From this estimate, a rough solar array sizing

was calculated. High-performance GaInP₂/GaAs/Ge cell technology was used with a conversion efficiency of 0.25, inherent degradation of 0.77, and annual environmental degradation of 2.75%. Mass of solar arrays was calculated at 12.1kg, with a required array surface area of 10.1m². In Figure 12, mission parameters are shown for the debris detumbling satellite. Calculations for solar array mass and sizing are shown in Figure 13.

Spacecraft and Mission Parameters		
Mdry	100 kg	spacecraft dry mass
<u>Mission Parameters</u>		
Dist to Sur	1.0 AU	Dist of S/C from Sun
G	1367 W/m ²	flux at S/C
Tm	1 yrs	mission life (siderial years)
<u>Daylight Performance</u>		
Pd	1900 W	daylight pow required
Td	60 min 1.000000 hrs	daylight period

Figure 12. Spacecraft and mission parameters necessary for solar array calculations

Solar Array Sizing		
Xd	0.8	S/A daylight trans efficiency
Xe	0.6	S/A eclipse trans efficiency
Psa	2375.0 W	daylight pow req.
Cell Type	GaInP2/GaAs/Ge	
η	0.25	cell (production) efficiency
α	1.2 kg/m ²	array specific mass
Id	0.77	Inherent degradation
θ	23.5 deg 0.410152 radians	cosine loss angle (worst case)
Yd	0.025 /yr	annual environmental deg rate
Ld	0.975000	lifetime degradation
P_o	341.8 W/m ²	Ideal pow output (per unit area)
P_BOL	241.4 W/m ²	BOL Pow prod capability (per unit area)
P_EOL	235.3 W/m ²	EOL Pow prod capability (per unit area)
A_sa	10.1 m ²	Required array size
PSA_BOL	2435.9 W	BOL pow output
M_sa	12.1 kg	Array mass
PSA_EOL	2375 W	EOL pow output

Figure 13. Solar array sizing calculations

Mission Mass Breakdown

System	Mass (kg)
Propulsion Subsystem	0.77
Propellant	9.96
Solar Array	12.1
Flywheel	75.0
Other spacecraft components	25.0
Total	122.8

Figure 14. Mass breakdown of different spacecraft calculated and assumed subsystems

As shown in Figure 14, a total mass of 122.8kg was calculated for the detumbling spacecraft, a relatively low mass for a satellite. With such a low mass, a fully-built spacecraft could be launched for as low as \$334,016 (using the Falcon 9, cited at \$2720/kg) (Jones, 2018).

3.3 Experimental System Design

To further study, validate, and optimize our mission design, we conducted two experiments which isolated specific systems within our design. The first experiment was a simulation of net capture in zero gravity. The simulation was created to provide a basis for further study on the finer details of net shape, materials, and launching parameters. The second experiment featured the use of a mechanical rig we built to emulate the use of a momentum wheel to control a rotating, captured body through a tether-net connection.

Net Simulation Design

The first phase in the use of tether-net systems is the launch and capture of target debris with a net; therefore the design of a net which reliably captures target debris is critical to the overall mission. There are many parameters involved in the design of a net, such as its shape, size, mass, & material. It is necessary to study the variables involved in net design before concluding an optimal design. Experiments performed in a gravitational environment are insufficient for observing how a particular net will operate. Zero gravity experiments in space and on parabolic

flights are ideal, but too costly for exploratory work. This leaves computer simulation as the best choice for low cost studies on the physics of net capture.

As all other papers on the simulations of net were either proprietary, or unavailable for public use, we choose to recreate the work of others from scratch. The goal of our project was to create an open source model of a net, which would provide a basis for future work on the design and simulation of different net properties. The minimum requirements for the simulation would be to model a net with sufficient accuracy such that changes in net parameters would properly affect some number of key characteristics in the simulation behavior. A single run of the simulation would feature the launch of the net towards a target object and demonstrate the collision and wrapping behavior of the net. See Figure 5 from Section 2.9 for a visual example of a simulated net used as inspiration.

We choose to use the mass spring model of a net for simulations. The mass spring model has been shown to work by others and is simple to implement. Background Section 2.9 discusses the mass spring model further. Figure 15 shows the shape and model of the net. All of the mass is contained in the individual nodes or cross sections. Nodes are connected together with spring damper constraints. The four corner nodes of the net are attached to an extra bullet node, which is larger in size and mass. The square configuration and number of nodes was standard across other papers, but could be changed in future iterations for further experiments.

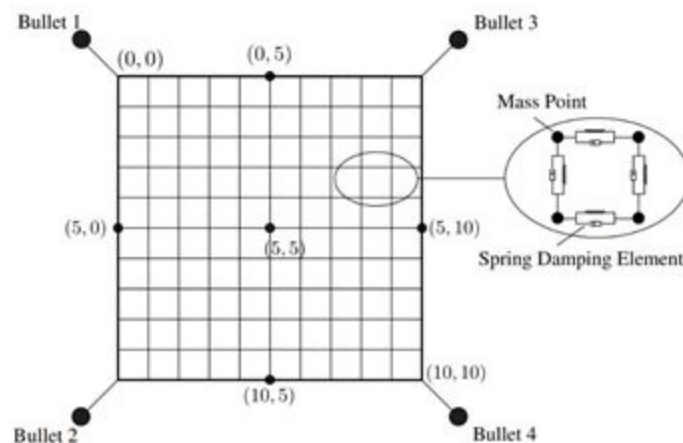


Figure 15. Geometric configuration of net from Shan, Guo, & Gill, 2018

The simulation was created using Bullet Physics. Bullet Physics is an open source library that handles collisions of rigid bodies and, soft bodies. It is fully programmable and features many options regarding constraints and system parameters. The accuracy and use of Bullet Physics as an engine was explored in de Jong's 2014 paper, *Simulating Rigid-Bodies, Strings and Nets*.

We modelled the target satellite as a simple rectangular prism. This was done for simplicity, and since the shape matched the physical experiment used for validation discussed below.

In order to optimize the design of the net, it was necessary to provide real-world data on a net's behavior against which to compare. A Vicon system³ allowed us to record positional data on a net dropped onto a stationary box. Figure 16 shows the setup used. A series of fourteen trackers were attached to the perimeter of the net, and a set of eleven Vicon cameras recorded the positions of the trackers over time while the net was dropped.



Figure 16. Physical net drop using Vicon cameras

³ <https://www.vicon.com/>

Tether-Net Experimental Design

Mechanical System Design

While momentum wheels are capable of transferring angular momentum to rigid systems, it is unsure whether a momentum wheel can successfully transfer momentum to a system when attached via a tether and net. Because of this a physical experiment was formulated to emulate the detumbling of space debris using a momentum wheel and tether-net connection. We built a rig that holds both an experimental chaser satellite and experimental space debris so that a momentum wheel and tether net connection for detumbling could be tested.



Figure 17. Physical Experiment

The experimental rig, Figure 17, consists a wooden frame that holds an experimental chaser satellite and an experimental space debris. The chaser sits on top of the frame and the space debris is situated directly below it. Both of these bodies sit on bearings, allowing them to rotate freely along the same axis. The two bodies can be connected via a tether and net, allowing different tether net configurations to be used. This allowed us to observe the effectiveness of a momentum wheel for slowing down space debris as well as observe the differences between various connection types for slowing down debris with a momentum wheel. The vertical

alignment of the chaser and space debris allow the effects of gravity to be minimized since gravity is acting along the same direction of the tension in the tether.

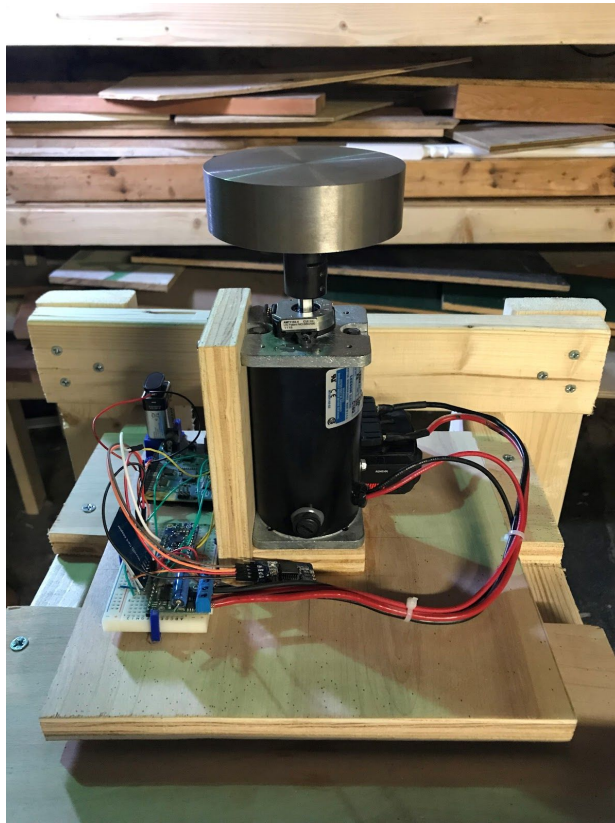


Figure 18. Chaser platform with motor and momentum wheel

The chaser satellite, Figure 18, is composed of a wooden platform with a small attachment point for a tether underneath that comes through the center of the bearing. Centered on the platform is an electric motor, powered by a 20 volt battery. An Arduino and electrical system controls the motor. A momentum wheel is attached on top of the motor. The momentum wheel is able to reach an angular velocity of 4000 rpm or 418.88 rad/s and has a moment of inertia of 0.001874 kgm^2 and mass of 1.696 kg. This gives it a potential angular momentum of 0.75 kgm^2/s . The wheel is used to apply a torque to the system as it is accelerated.



Figure 19. Debris platform

The space debris, Figure 19, consists of wooden platform with a 6.8 kg cylindrical weight centered on it. The platform sits atop a bearing allowing it to freely rotate. An attachment point for a tether is located in the center of the platform. Different weights are able to be used for the space debris.

Electrical System Design

The electrical system reads data from multiple external sensors and controls a motor to detumble the debris in our experiment. We decided to use the Arduino due to its simplicity and ease of programming. Because the Arduino Uno has no external memory, an SD-card reader/writer was necessary to output data. After our initial experiments, it became clear that, to match the data from the chaser and target, we would need to implement a real-time clock to sync the data. The power draw of the system is 0.5A at 20V, for a total of 9.0W with an efficiency of 0.9.

Chaser Electrical System

The chaser electrical system consists of an Arduino Uno, Adafruit LSM9DS1 9-axis inertial measurement unit, Pololu high-power motor driver, DS3231 real-time clock, and an SPI SD-card reader and writer. The wiring is shown in the image below.

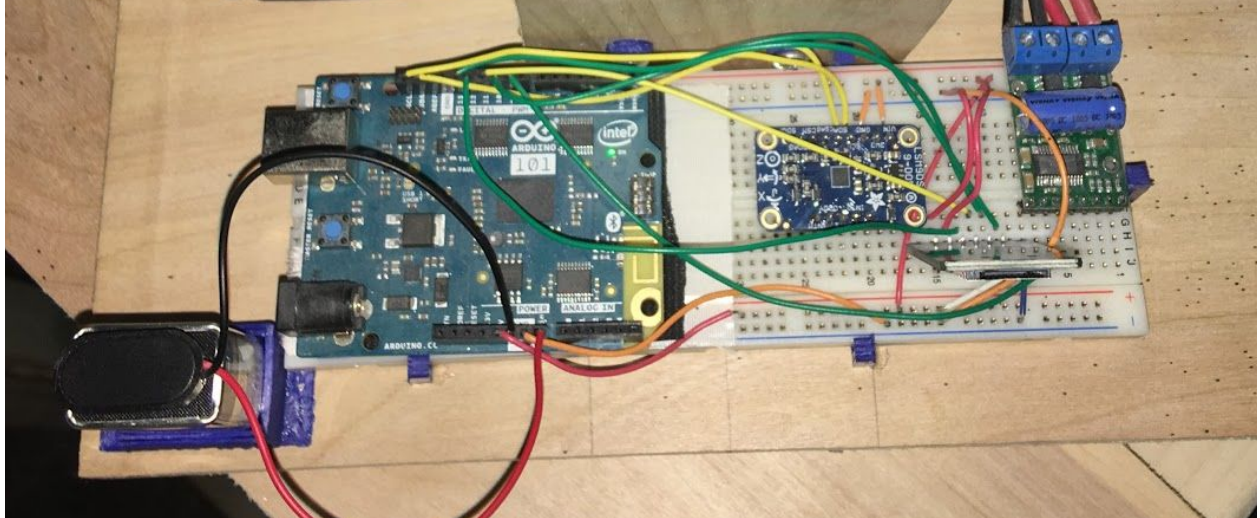


Figure 20. Chaser electrical system

Target Electrical System

The target electrical system consists of an Arduino Uno, Adafruit LSM9DS1 9-axis inertial measurement unit, DS3231 real-time clock, and an SPI SD-card writer. The wiring is the exact same as the chaser without the motor driver.

Software Design

For both the chaser and target, the software wrote the data from the experiment to the SD card. Using data from the real-time clocks on each, the two datasets could then be matched in post-processing and graphs were made. After our initial experiments, we found that the 350 degrees/sec was a good trigger speed for the Arduino and flywheel to speed up in time for the peak of the curve. From there, an acceleration and maximum speed for the flywheel was calculated using the moment of inertia of the debris.

Target Software Design

The software design for the chaser involves the Arduino reading data from the gyroscope and real-time clock, waiting for the speed to reach 350 deg/sec then activating the motor routine, which accelerates the flywheel to 8400 deg/sec from rest. A model of the system is shown below.

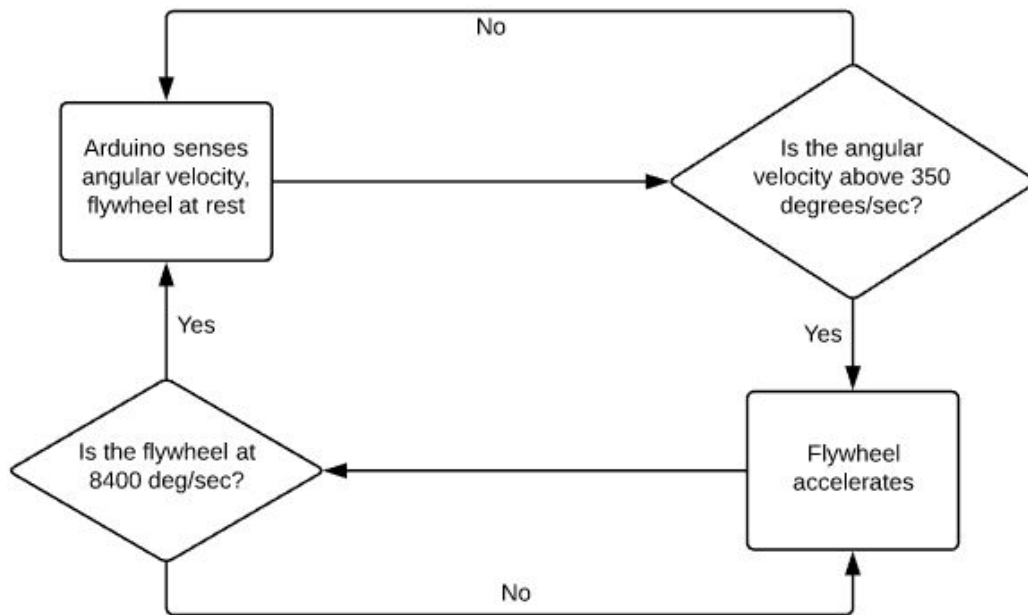


Figure 21. Flowchart diagram of chaser software design

Target Software Design

The software design for the target was slightly different from the chaser, as the goal of the target system was just to record the rotational speed of the target. In the target program, the Arduino read data from the gyroscope and real-time clock. Unlike the chaser software system, the target software system does not make any calculations and has no external sensors, so no flowchart is required to describe the system.

4 Experimental Results

4.1 Net Simulation Experiment

The first task was to record data on real world nets. The procedure for this experiment was described further in design Section 3.3. Figure 22 shows the labeled trial used for validation. Individual nodes were manually labeled, with the help of a video recording done at the time of the trial. Gaps in the trial data were filled using the cyclic filling algorithm in Vicon Nexus.

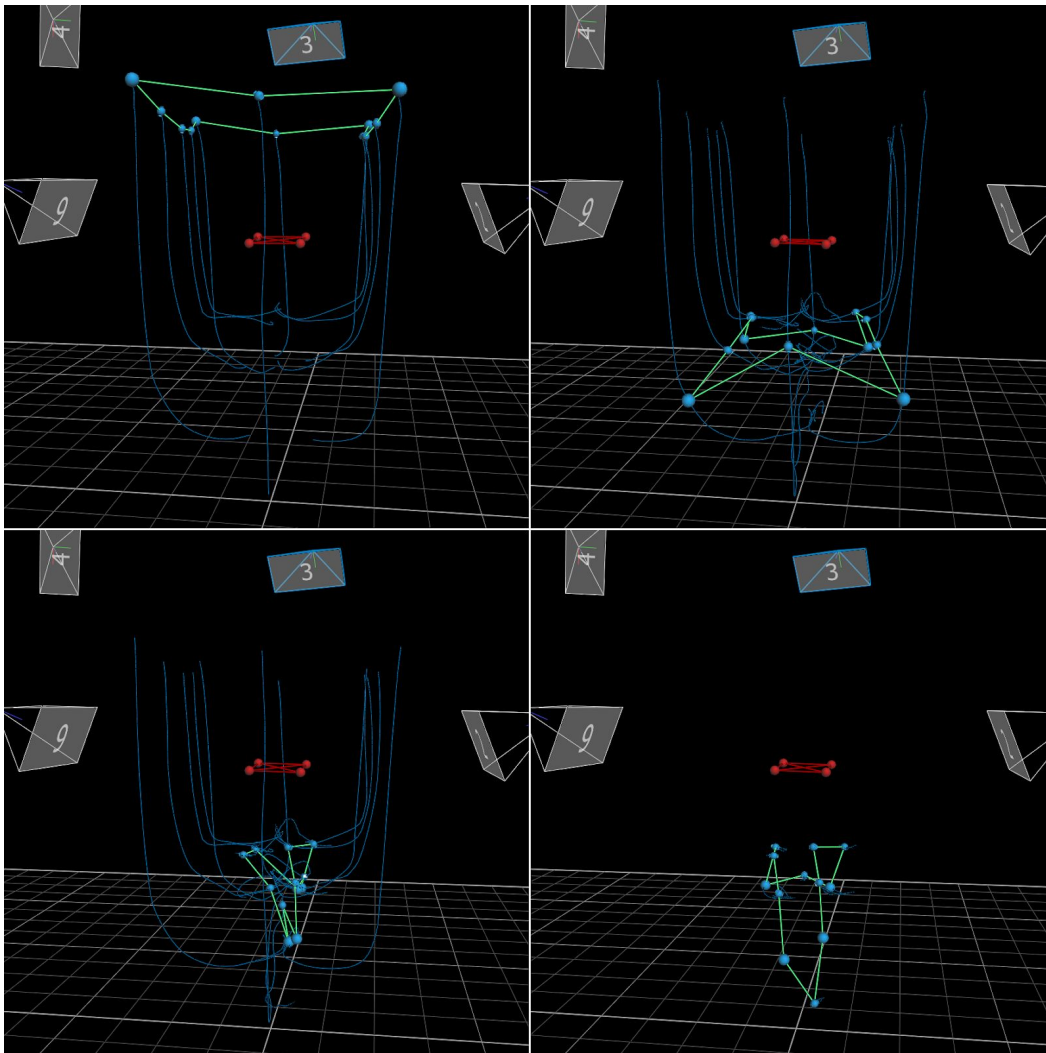


Figure 22. Screenshots of tracked net positions at frames 550, 610, 670, and 870

From this data, a simulation was created in Bullet Physics that matched the initial spatial parameters. A run of this trial is shown below.

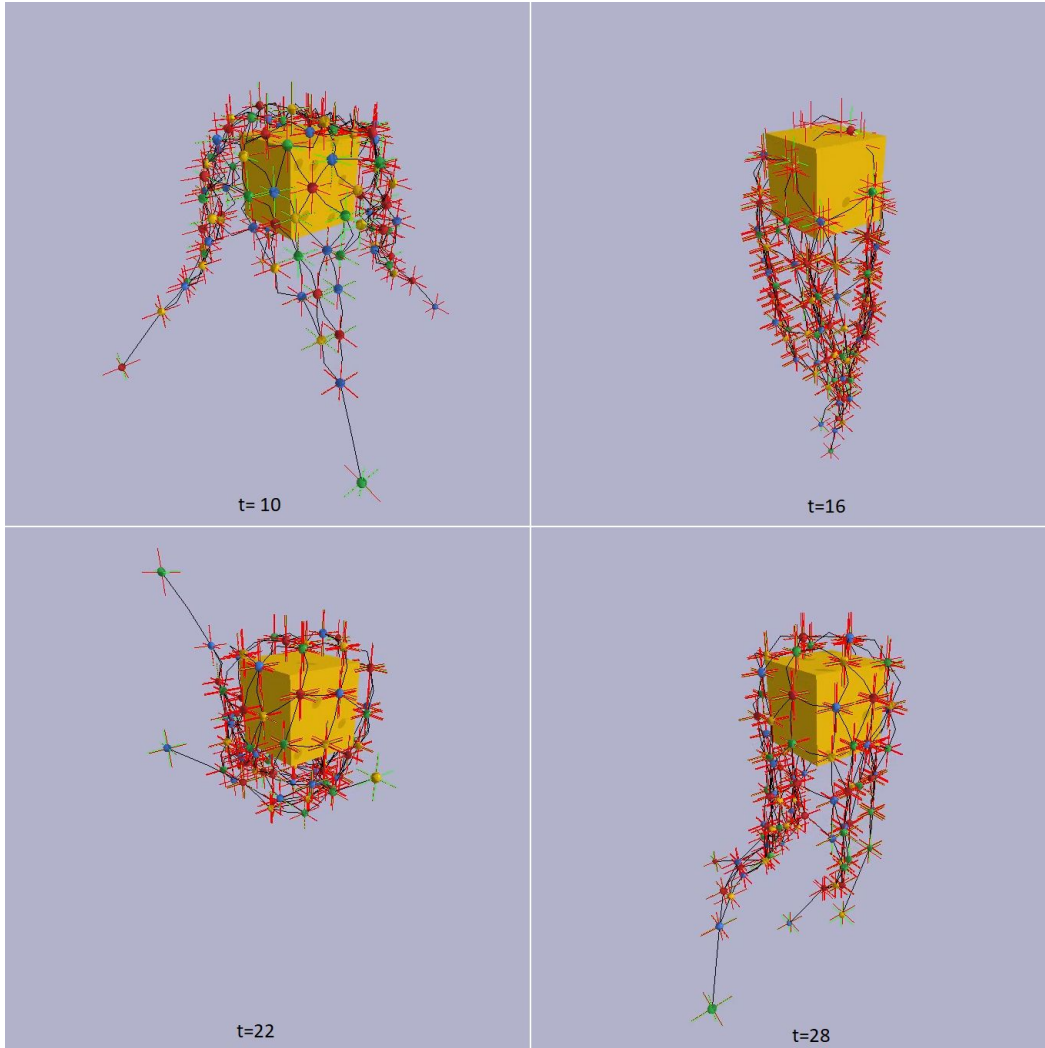


Figure 23. Screenshots of Bullet Physics Simulation with gravity

Adjustments were made on the Bullet Physics simulation to minimize the deltas between x and y positions over time. This comparison was done in excel, by exporting the positional values from Bullet Physics and Vicon Nexus and using the difference in positions along each axis. The stiffness and masses of nodes were adjusted to minimize these deltas through trial and error.

The final simulation uses the updated parameters from the optimization procedure, but operates without gravity, and on a rotating debris. The mass of the debris was set to 4000kg, compared to the total mass of 54 kg across the entire net. Figure 24 shows screenshots of the final simulation.

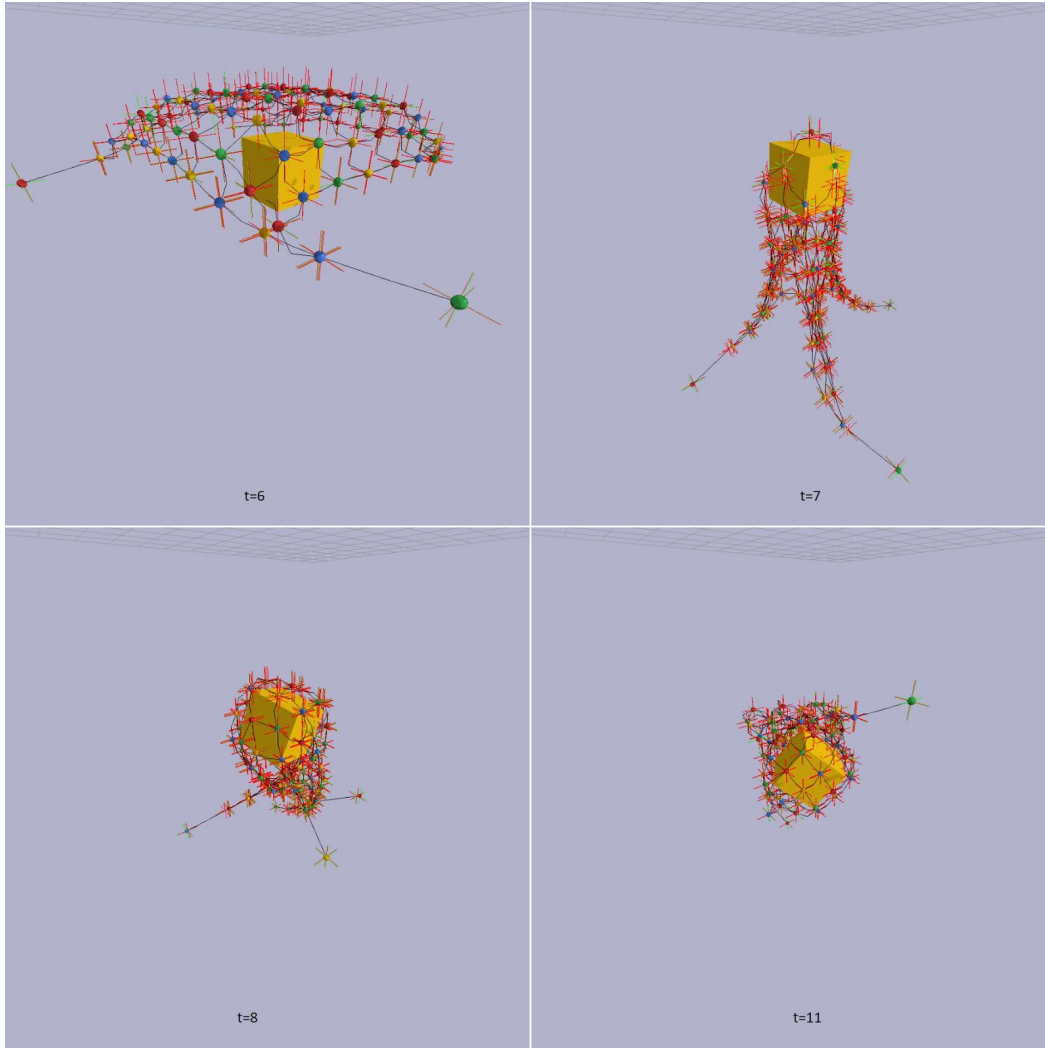


Figure 24. Screenshots of Final Bullet Physics Simulation, showing successful capture of rotating target debris in zero gravity

4.2 Tether-Net Experiment

Setup

The following four tests were conducted using the physical experiment detailed in the Tether-Net Experimental Design chapter, Section 3.3. The main goal of these tests was to compare the detumbling of space debris using different connection methods with a momentum wheel. Another goal was to compare the behavior of the debris detumbling with the momentum wheel powered with having the system slow down on its own.

- Detumbling of debris using a momentum wheel and rigid connection. For this test the chaser and debris were attached rigidly.

- Detumbling of debris using a momentum wheel and tether connection. For this test the chaser and debris were connected via a steel cord.
- Detumbling of debris using a momentum wheel and tether-net connection. For this test a steel cord was attached to the chaser with the other end being attached to a net that wrapped around the debris.
- Detumbling of debris using air resistance and friction. For this test the system was allowed to slow down on its own from drag and friction in the bearings.

For each test the debris was spun up to speed by hand. For the first three tests that used the momentum wheel to detumble the debris, the momentum wheel was activated once the chaser platform reached an angular velocity of 350 deg/sec. The momentum wheel would then accelerate at 2184 deg/sec² to a final angular velocity of 8,400 deg/sec.

4.3 Results and Discussion

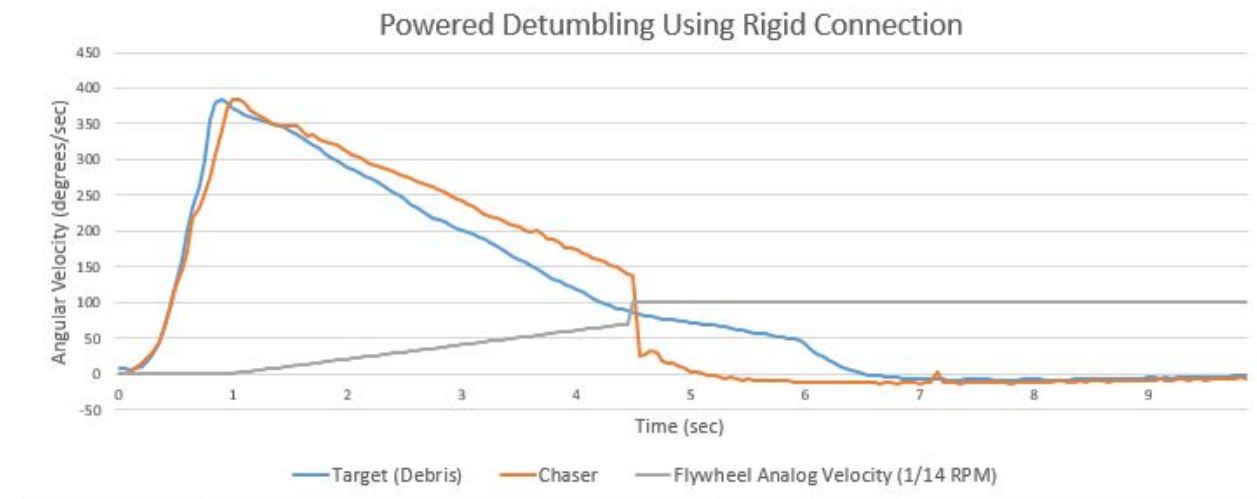


Figure 25. Graph of experimental test of powered detumbling using rigid connection

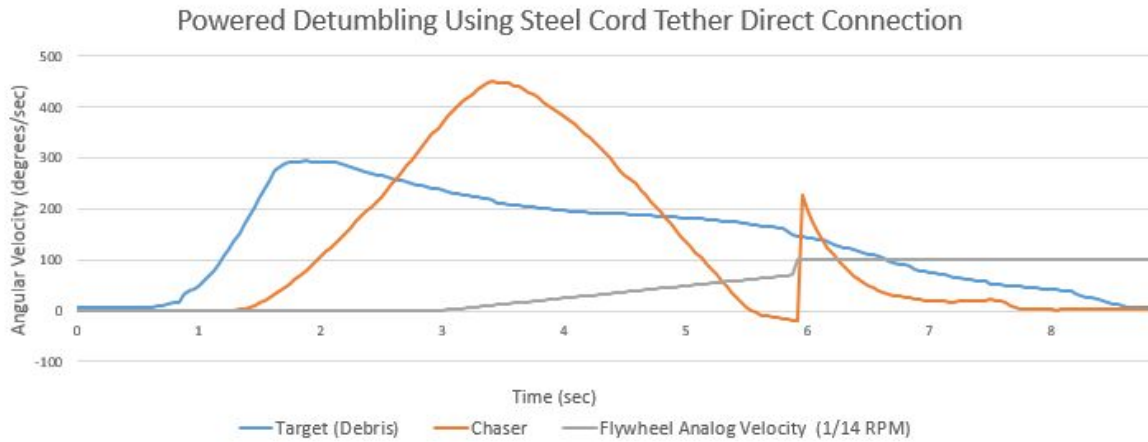


Figure 26. Graph of experimental test of Powered Detumbling using Steel Cord Tether

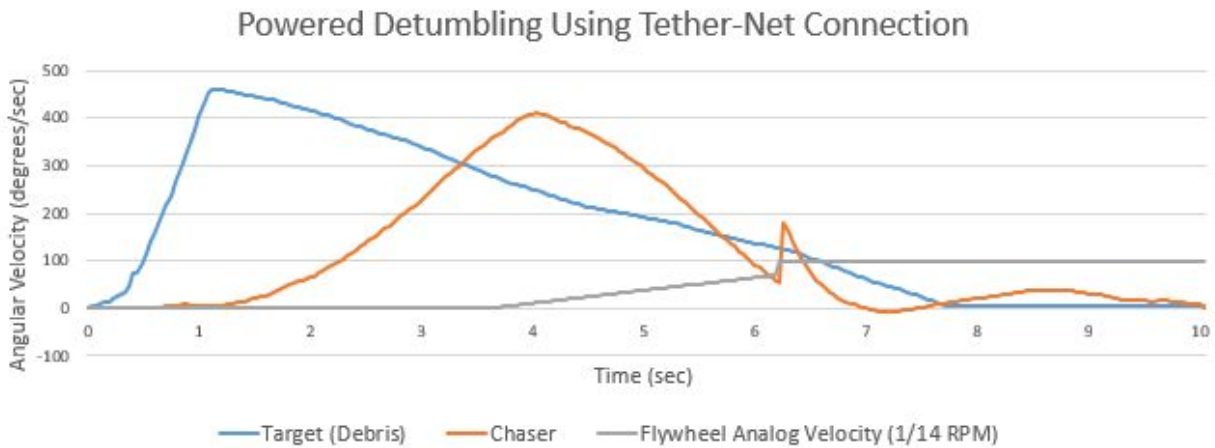


Figure 27. Graph of experimental test of powered detumbling using tether-net connection

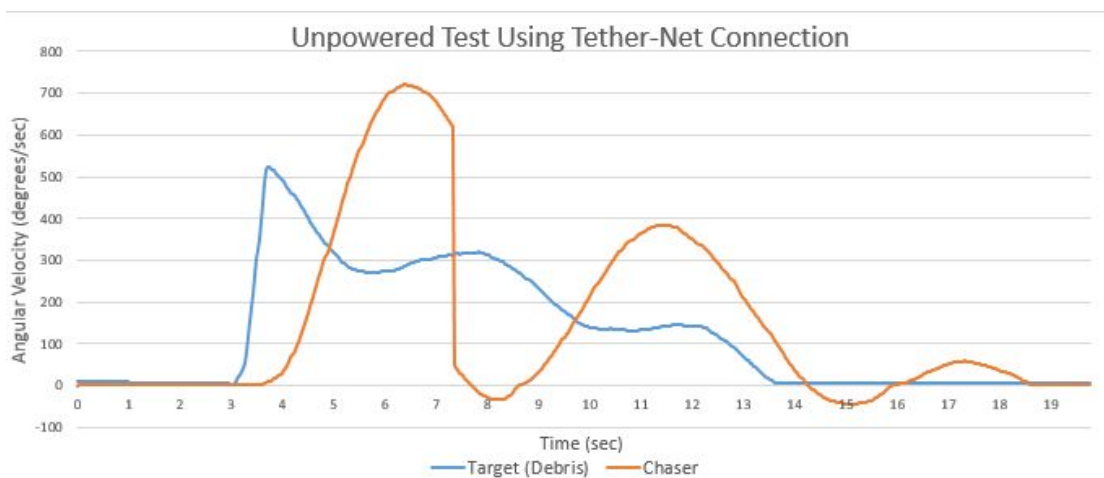


Figure 28. Graph of experimental test of unpowered test using tether-net connection

Compared to the unpowered test using a tether-net connection, the powered tether-net connection slowed down quicker and in a more stable manner. In the unpowered tether-net graph, Figure 28, the second peak of the chaser velocity represents an oscillation of the chaser. As the wind up in the tether is released, it effects the chaser much more strongly because the chaser has a much lower moment of inertia compared to the debris. This is what causes the second peak. This second oscillation is not present in the powered tether-net connection test, Figure 27. There is a second spike in the angular velocity, but this is caused by a second burst of acceleration of the momentum wheel, which can be seen on the grey line. This second burst of acceleration from the motor was added to deal with the consequences of the wind up in the tether. Without this second burst the chaser would oscillate similar to the unpowered test, but the second stage in the wheel's acceleration allows it to counteract this release of tension in the tether. These tests show the possibility of controlling a piece of tumbling debris with a tether-net connection and momentum wheel.

The addition of the net in a tether connection dampens the forces being transmitted through the connection in the system. This can be seen when comparing the powered tether-net connection, Figure 27, and powered tether connection graphs, Figure 26. The chaser accelerates faster and sooner from the spin of the debris in the tether connection test when compared to the tether-net. This is something that should be considered when dealing with a net capture method for space debris remediation. The damping effect of a net could be significant when applied in space. The degree in which the net dampens forces depends on the net material and configuration. It also depends on uncontrollable variables such as how well the net captures the debris. Therefore, the damping effect of the net will vary from capture to capture.

The rigid connection test shows the increased amount of control that a rigid connection gives compared to a tether or tether-net connection. The angular velocity of both the chaser and debris follow a very similar path as they slow down, shown in Figure 25. The small difference in the two velocities can be due to the connection in the experiment not being truly rigid. A perfectly rigid connection would produce the exact same velocities. A perfectly rigid connection would probably not exist in the real world because of the flexing of materials in the connection device and in the satellite bodies.

As mentioned in the comparison between the powered and unpowered tether-net connection tests, the wind up in the tether plays a key role in the stability of the system. If a chaser is detumbling a piece of space debris with a much higher mass, the chaser will be more vulnerable to the sudden release of wind up in the tether. This is the reason why in the experiment a second acceleration of the momentum wheel was added, to counteract this release. As mentioned in the background, momentum wheels are capable of accurate control over satellite movement, it is feasible that having a reactionary momentum wheel that reacts to the forces in the tether to control the detumbling of space debris would be able to detumble with a good degree of control.

These tests are limited in conveying an accurate detumbling of space debris in orbit using a chaser satellite with a tether-net capture method and momentum wheel for detumbling. One reason is the fixed axis. In this test, it is assumed that the chaser and debris are both rotating along the same axis and that this axis does not shift during detumbling. In a real space detumbling environment, the axis of rotation of both the chaser and debris will shift and not always line up. This test also assumes a constant tension in the tether since the chaser and debris are a fixed length apart. In an actual detumbling mission, the tether tension is something that will need to be controlled. In the tests, the debris was spun up by hand, resulting in different initial angular velocities. This could potentially cause inaccuracies in the conclusions drawn. There are other important factors in detumbling that this experiment does not address. One example is the forces the tether and net are experiencing and the possibility of either element snapping.

5 Concluding Remarks

5.1 Conclusions

In this Major Qualifying Project, we designed a mission framework to detumble and deorbit five separate satellites in order to stabilize the debris density in low Earth orbit (LEO). The calculations in mission design provided a hypothetical set of parameters and materials that could be used for a mission. In addition, we performed exploratory experiments relevant to essential mission phases to show proof of concepts needed for the use of tether-nets in detumbling of space debris. Our physical experiment proved the viability of momentum wheels in the controlled detumbling of space debris and explored the potential effect of tether stiffness. The simulated experiments verified existing research on the effectiveness of nets to capture rotating debris and furthermore provided an open source code-base for future work to reference and improve.

5.2 Lessons Learned

The goal of this project was to understand, develop, and validate a mission framework for a satellite designed to detumble spinning satellites using the tether-net methodology. From the simulations, we learned that the mass-spring damper model of a net has limitations for simulations beyond capture dynamics, specifically pertaining to friction from rotation of the net and the resultant forces. From experimentation, it was learned that adding a reactionary element to the momentum wheel system would be very beneficial in adding extra control over detumbling the debris. Also, rigid connections offer a more accurate transmission of forces during the detumbling process. Finally, having a net tends to dampen the forces transmitted by a tether.

When building and running the experiment, we found that a simple system was the most effective at collecting data. As the complexity of the system increased, time for testing increased almost exponentially, to the point where, towards the end of our experimentation, each test took nearly an hour to record. In the future, simpler experimental design would allow for more painless data collection. Finally, we learned that these systems have a tendency to break, and constant vigilance and original build quality are essential to continuous data collection.

5.3 Suggested Future Work

There are many steps that can be taken to continue the work described in this paper. Further work on this project would expand on the experimentation and testing of the tether-net linkage as well as validation of the mission framework in microgravity or in simulation.

While the tests conducted by the team covered a basic proof of concept of the tether-net linkage for detumbling, further testing could prove the methodology with higher accuracy. Further development of the experiment described in the Tether-Net Experimental Design, Section 3.3, portion of this report would include a reliable mechanism for the initial spinning of the debris (in this experiment approximate torque was estimated by pushing the debris manually). Additionally, different tether and net materials and configurations could be tested for their ability to detumble debris. With more accurate measuring techniques specific tether materials could be compared as well. Our current data points to the conclusion that rigid tethers have more control and stability when detumbling debris, while more elastic tethers cause a lag that creates high spin rates in the chaser and needs a more complicated detumbling procedure.

Additionally, the detumbling method using a momentum wheel has the need to be validated in lower-friction environments. Though the ideal environment is in microgravity, other Earth-based experimental techniques are cheaper, simpler next steps. Low-friction, Earth-based options include air bearings, magnetic bearings, or parabolic flights. The ability to create a momentum wheel system that is dependent on reacting to the torque and tension in the tether should also be researched.

Works Cited

- Aslanov, V., & Yudinsev, V. (2013). Dynamics of large space debris removal using tethered space tug. *Acta Astronautica*, 91, 149–156. <https://doi.org/10.1016/j.actaastro.2013.05.020>
- Benvenuto, R., & Lavagna, M. (2013). Flexible capture devices for medium to large debris active removal: simulations results to drive experiments. In *12th Symposium on Advanced Space Technologies in Automation and Robotics* (pp. 1–8). ASTRA Noordwijk, The Netherlands.
- Benvenuto, R., Lavagna, M., & Salvi, S. (2016). Multibody dynamics driving GNC and system design in tethered nets for active debris removal. *Advances in Space Research*, 58(1), 45–63. <https://doi.org/10.1016/j.asr.2016.04.015>
- Bombardelli, C., and Pelaez, J., “Ion Beam Shepherd for Contactless Space Debris Removal,” *Journal of Guidance, Control, and Dynamics*, vol. 34, May 2011, pp. 916–920.
- Botta, E. M., Sharf, I., Misra, A. K., & Teichmann, M. (2016). On the simulation of tether-nets for space debris capture with Vortex Dynamics. *Acta Astronautica*, 123, 91–102. <https://doi.org/10.1016/j.actaastro.2016.02.012>
- Cao, D. Q., & Tucker, R. W. (2008). Nonlinear dynamics of elastic rods using the Cosserat theory: Modelling and simulation. *International Journal of Solids and Structures*, 45(2), 460–477. <https://doi.org/10.1016/j.ijsolstr.2007.08.016>
- de Jong, J. H., Wormnes, K., and Tiso, P., “Simulating Rigid-Bodies, Strings and Nets for Engineering Applications Using Gaming Industry Physics Simulators,” p. 8.
- Edelbaum, T. N., “Edelbaum, T. N., ‘Propulsion Requirements for Controllable Satellites,’ ARSJ, Aug. 1961, pp. 1079–89,” ARSJ, Aug. 1961, pp. 1079–89.
- Gaposchkin, E. M. (1994). *Calculation of satellite drag coefficients*. MASSACHUSETTS INST OF TECH LEXINGTON LINCOLN LAB.
- Gołębiowski, W, Michalczyk, R., Battista, U., Dyrek, M., Derda, Z., & Wormnes, K. (2014). Reliable and Efficient Simulation of Nets for Active Space Debris Removal Purposes, 8.
- Gołębiowski, Wojciech, Michalczyk, R., Dyrek, M., Battista, U., & Wormnes, K. (2016). Validated simulator for space debris removal with nets and other flexible tethers applications. *Acta Astronautica*, 129, 229–240. <https://doi.org/10.1016/j.actaastro.2016.08.037>
- Gómez, N. O., & Walker, S. J. I. (2015). Earth’s gravity gradient and eddy currents effects on the rotational dynamics of space debris objects: Envisat case study. *Advances in Space Research*, 56(3), 494–508. <https://doi.org/10.1016/j.asr.2014.12.031>
- Huang, P., Zhang, F., Chen, L., Meng, Z., Zhang, Y., Liu, Z., & Hu, Y. (2018). A review of space tether in new applications. *Nonlinear Dynamics*, 94(1), 1–19. <https://doi.org/10.1007/s11071-018-4389-5>

- Hughes, P. (1986). *Spacecraft Attitude Dynamics*. Dover Publications. Retrieved from <https://app.knovel.com/hotlink/pdf/id:kt00B7VER2/spacecraft-attitude-dynamics/spacecraft-torques>
- Ives, N. E. (1963). *The effect of solar radiation pressure on the attitude control of an artificial earth satellite*. Citeseer.
- Imburgia, J. S., "Space Debris and Its Threat to National Security: A Proposal for a Binding International Agreement to Clean up the Junk," *Vanderbilt Journal of Transnational Law*, vol. 44, 2011, p. 589.
- Johnson, N. (2011). USA Space Debris Environment, Operations and Policy Updates. *48th Session of the Scientific and Technical Subcommittee Committee on the Peaceful Uses of Outer Space, United Nations*, 7–18.
- Jones, H., "The Recent Large Reduction in Space Launch Cost," Jul. 2018.
- Kessler Donald J., & Cour-Palais Burton G. (2012). Collision frequency of artificial satellites: The creation of a debris belt. *Journal of Geophysical Research: Space Physics*, 83(A6), 2637–2646. <https://doi.org/10.1029/JA083iA06p02637>
- Krishnan, H., McClamroch, N. H., and Reyhanoglu, M., "Attitude stabilization of a rigid spacecraft using two momentum wheel actuators," *Journal of Guidance, Control, and Dynamics*, vol. 18, Mar. 1995, pp. 256–263.
- "LEGEND – a three-dimensional LEO-to-GEO debris evolutionary model," *Advances in Space Research*, vol. 34, Jan. 2004, pp. 981–986.
- Liou, J.-C., "An active debris removal parametric study for LEO environment remediation," *Advances in Space Research*, vol. 47, Jun. 2011, pp. 1865–1876.
- Liou, J.-C., "Engineering and technology challenges for active debris removal," *Progress in Propulsion Physics*, St. Petersburg, Russian: EDP Sciences, 2013, pp. 735–748
- Medina, A., Cercós, L., Stefanescu, R. M., Benvenuto, R., Pesce, V., Marcon, M., ... Wormnes, K. (2017). Validation results of satellite mock-up capturing experiment using nets. *Acta Astronautica*, 134, 314–332. <https://doi.org/10.1016/j.actaastro.2017.02.019>
- O'Connor, W. J., & Hayden, D. J. (2017). Detumbling of Space Debris by a Net and Elastic Tether. *Journal of Guidance, Control, and Dynamics*, 40(7), 1832–1836. <https://doi.org/10.2514/1.G001838>
- Pulliam, W. (2011). *Catcher's Mitt Final Report*. DEFENSE ADVANCED RESEARCH PROJECTS AGENCY ARLINGTON VA, United States.
- Shan, M., Guo, J., & Gill, E. (2016). Review and comparison of active space debris capturing and removal methods. *Progress in Aerospace Sciences*, 80, 18–32. <https://doi.org/10.1016/j.paerosci.2015.11.001>
- Shan, M., Guo, J., & Gill, E. (2017). Deployment dynamics of tethered-net for space debris removal. *Acta Astronautica*, 132, 293–302. <https://doi.org/10.1016/j.actaastro.2017.01.001>
- Shan, M., Guo, J., & Gill, E. (2018). Contact Dynamics on Net Capturing of Tumbling Space Debris. *Journal of Guidance, Control, and Dynamics*, 41(9), 2063–2072. <https://doi.org/10.2514/1.G003460>

- Sharf, I., Thomsen, B., Botta, E. M., and Misra, A. K., "Experiments and simulation of a net closing mechanism for tether-net capture of space debris," *Acta Astronautica*, vol. 139, Oct. 2017, pp. 332–343.
- Tsiotras, P., Shen, H., and Hall, C., "Satellite Attitude Control and Power Tracking with Energy/Momentum Wheels," *Journal of Guidance, Control, and Dynamics*, vol. 24, Jan. 2001, pp. 23–34.
- "USA Space Debris Environment, Operations, and Policy Updates", UNOOSA, Available: <http://www.unoosa.org/>.
- Wang, B., Meng, Z., & Huang, P. (2017). Attitude control of towed space debris using only tether. *Acta Astronautica*, 138, 152–167. <https://doi.org/10.1016/j.actaastro.2017.05.012>
- Wertz, J., Everett, D., and Puschell, J., *Space Mission Engineering: The New SMAD*, Microcosm Press, 2011.
- Wormnes, K., Letty, R. L., Summerer, L., Schonenborg, R., Dubois-Matra, O., Luraschi, E., Delaval, J. (2013). ESA TECHNOLOGIES FOR SPACE DEBRIS REMEDIATION, 8.
- Yang, L., Zhang, Q., Zhen, M., & Liu, H. (2017). *Dynamics and Design of Space Nets for Orbital Capture*. Springer.
- Zhao, Y., Huang, P., and Zhang, F., "Capture Dynamics and Net Closing Control for Tethered Space Net Robot," *Journal of Guidance, Control, and Dynamics*, Sep. 2018, pp. 1–10.
- Zhao, Y., Huang, P., & Zhang, F. (2018). Capture Dynamics and Net Closing Control for Tethered Space Net Robot. *Journal of Guidance, Control, and Dynamics*, 1–10. <https://doi.org/10.2514/1.G003672>